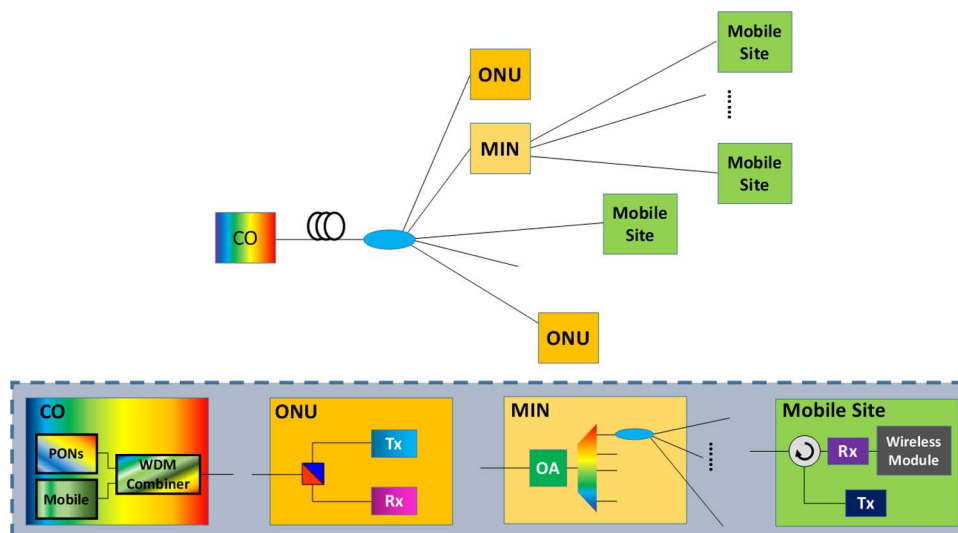


# Cost-Effective Mobile Backhaul Network Using Existing ODN of PONs for the 5G Wireless Systems

Volume 7, Number 6, December 2015

Jiun-Yu Sung  
Chi-Wai Chow, Senior Member, IEEE  
Chien-Hung Yeh  
Yang Liu  
Gee-Kung Chang, Fellow, IEEE



DOI: 10.1109/JPHOT.2015.2497222  
1943-0655 © 2015 IEEE

# Cost-Effective Mobile Backhaul Network Using Existing ODN of PONs for the 5G Wireless Systems

Jiun-Yu Sung,<sup>1</sup> Chi-Wai Chow,<sup>1</sup> *Senior Member, IEEE*, Chien-Hung Yeh,<sup>2</sup> Yang Liu,<sup>3</sup> and Gee-Kung Chang,<sup>4</sup> *Fellow, IEEE*

<sup>1</sup>Department of Photonics and Institute of Electro-Optical Engineering, National Chiao Tung University, Hsinchu 30010, Taiwan

<sup>2</sup>Department of Photonics, Feng Chia University, Taichung 40724, Taiwan

<sup>3</sup>Philips Electronics Ltd., NT, Hong Kong

<sup>4</sup>School of Electrical and Computer Engineering, Georgia Institute of Technology, Atlanta, GA 30308 USA

DOI: 10.1109/JPHOT.2015.2497222

1943-0655 © 2015 IEEE. Translations and content mining are permitted for academic research only.

Personal use is also permitted, but republication/redistribution requires IEEE permission.

See [http://www.ieee.org/publications\\_standards/publications/rights/index.html](http://www.ieee.org/publications_standards/publications/rights/index.html) for more information.

Manuscript received October 19, 2015; revised October 28, 2015; accepted October 29, 2015. Date of publication November 4, 2015; date of current version December 11, 2015. This work was supported in part by the Taiwanese Ministry of Science and Technology under Grant MOST-104-2628-E-009-011-MY3, Grant MOST-103-2221-E-009-030-MY3, and Grant MOST 103-2218-E-035-011-MY3; by the Aim for the Top University Plan, Taiwan; and by the Taiwanese Ministry of Education. Corresponding author: Y. Liu (e-mail: yliu.terse@gmail.com).

**Abstract:** An optical distribution network (ODN) sharing scheme to integrate mobile backhaul networks with the existing passive optical network (PON) systems is proposed and demonstrated. With the ODN sharing scheme, the expense of building new fibers for the next-generation fifth-generation (5G) mobile backhaul networks can be reduced. As many wavelengths are allocated to the already deployed PON systems, there remain limited wavelengths for the mobile backhaul systems. Hence, to efficiently increase the serving cell sites of the 5G systems, spectral-efficient orthogonal frequency-division multiplexing (OFDM) is adopted in the mobile backhaul systems. In order to reduce the latency of the system, adaptive adjustment of the OFDM signals for different transmission distances is averted. The OFDM signals are transmitted only using specific available bandwidth. The available bandwidth for each wavelength is studied according to the power fading relationship between the transmission distances and the chirp induced from signal modulation. A proof-of-concept demonstration experiment has been performed. In our results, 20.17 Gb/s with a bit error rate (BER) lower than  $3.8 \times 10^{-3}$  was realized with a split ratio of 256 and a 40-km transmission distance of the PON ODN. Hence, each wavelength can support about 20, six, and two nodes for the IMT-advanced, current Long-Term Evolution-Advanced (LTE-A) systems, and the expected 5G systems, respectively.

**Index Terms:** Optical communication, passive optical network (PON), fiber optic communication, mobile backhaul.

## 1. Introduction

Prosperous development of smart devices pushes the evolution of the mobile communication techniques. While fourth-generation (4G) techniques have become more mature recently, it is then reasonable to investigate the challenges of fifth-generation (5G) wireless networks to meet the bandwidth demand of mobile data services. The predicting features of the 5G systems

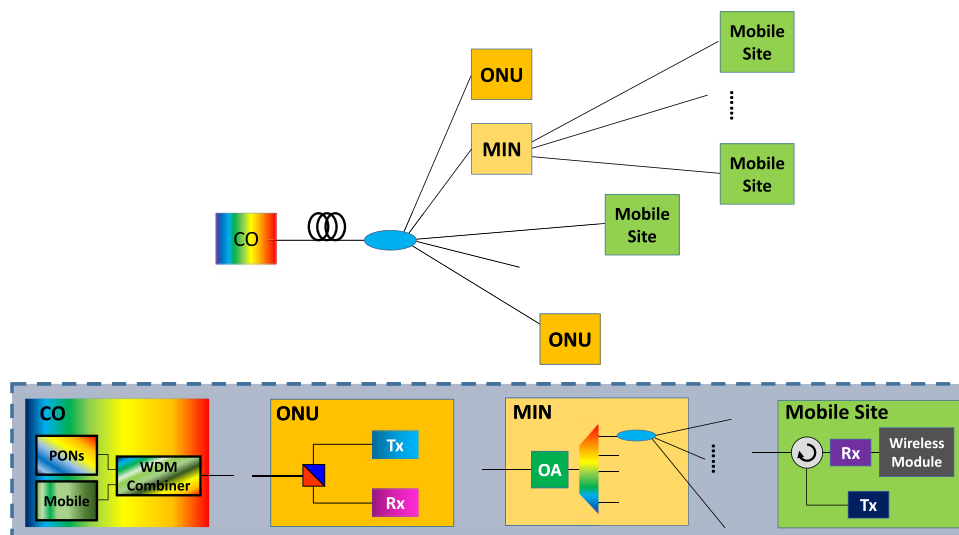


Fig. 1. Proposed architecture to integrate the mobile backhaul network with the existing PON. CO: central office; MIN: mobile intermediate node; OA: optical amplifier; ONU: optical network unit.

includes 1000 folds of the capacity density of the 4G systems, peak capacity of tens of Gigabits per second, and efficiency improvement [1], [2]. To meet the high capacity density requirement, deploying massive small cells is inevitable. Optical fibers have the characteristics of high bandwidth and low transmission loss; hence it is beneficial to use optical fibers as the transmission media between the mobile sites and their central office (CO). Though optical fibers can provide sufficient bandwidth and transmission distance for the mobile backhaul networks, deploying new fibers is costly [3]. In the early stage of 5G development, it is uncertain if these deployment cost can be balanced in acceptable time ranges. Hence, looking for economical schemes for the 5G mobile backhaul networks are important.

Passive optical networks (PONs) were widely deployed in the last decade [4], [5]. By using the existing PON systems, the deployment cost of the backhaul networks can be reduced in the trial stage of the 5G systems. However, since many wavelengths are allocated to the already deployed PON systems [6], the available wavelengths for the mobile backhaul systems are highly limited. Hence, to meet the capacity requirement of the 5G systems, high spectral efficiency modulation technique is very important.

Orthogonal frequency-division multiplexing (OFDM) is a modulation technique featuring in high spectral efficiency and dispersion resistance [7]. Through the OFDMA wireless access technique, OFDM may also be suitable as an intermediate system between the 4G and 5G era, for which different data rates may be required for the corresponding backhaul systems. Techniques of the OFDM systems were extensively investigated [8]–[12]. Although OFDM can provide higher spectral efficiency, its useful bandwidth is still limited by the chromatic dispersion of a fiber. In ref. [11], two wavelengths carrying the same data with modulators having different chirp values were adopted to fully use the photo-diode (PD) bandwidth over different distances. However, this may cause waste of the wavelengths. In ref. [12], adaptive band allocation, sub-carrier loading, and power loading techniques are used to optimize the subcarrier signals for different transmission distances. Hence, high data rate can be realized. While tremendous new cells located at different distances from the CO are introduced, more complex calculation at the transmitter end are required to compensate the dispersion-induced power fading and to bit-load the OFDM subcarriers. This can increase both the system cost and the process latency.

In this paper, an optical distribution network (ODN) sharing scheme is proposed to integrate the mobile backhaul systems into the existing PON systems. By efficiently using the deployed ODN, the expenses of building new fibers for the mobile backhaul network can be reduced. The system bandwidth is determined by analyzing the power fading behavior within 40 km

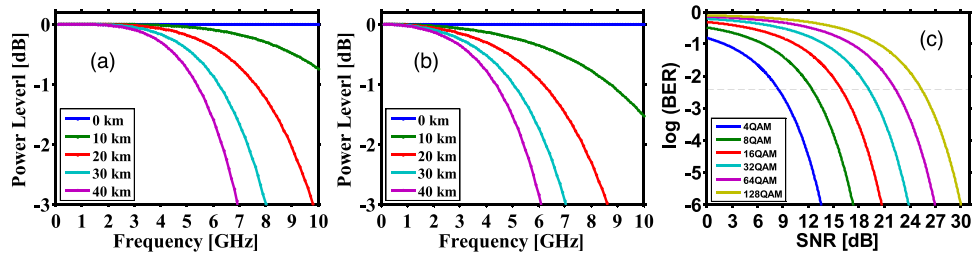


Fig. 2. Signal analyses. (a) and (b) Power response after different transmission distances. (a) Chirp = 0; (b) chirp = 0.2. (c) Relationship between BER and SNR.

transmission to meet the requirement of the second stage next generation PON (NG-PON2). The 3-dB bandwidth available after 40 km transmission is used for all OFDM signals. Hence, it is not necessary to adaptively adjust the OFDM signals according to the transmission distances. High data rate and low process time can thus be achieved. 20.17 Gb/s net data rate with bit error rate (BER) less than  $3.8 \times 10^{-3}$  was demonstrated over a PON ODN with 256 split ratio and 40 km transmission distance, which meets the requirement of NG-PON2. In our results, 20, six, and two end nodes can be supported by each wavelength, respectively, for the requirements of IMT-Advanced (IMT-A) [14], LTE-Advanced (LTE-A) [15], and what is expected of 5G [1], [2].

## 2. Architecture and Numerical Analyses

Fig. 1 shows our proposed architecture to integrate the mobile backhaul network with the existing PON. The PON systems and the mobile systems share the same CO. Data of different services are transmitted using optical carriers with different wavelengths. A wavelength-division-multiplexing (WDM) combiner is used to combine the data streams of different services in the CO, as shown in inset of Fig. 1. The signals are distributed through the ODNs of the existing PON systems. The optical network units (ONUs) of the PON systems are connected with the end terminals of the ODN and received the PON data. Some mobile intermediate nodes (MINs) are also connected to the terminal nodes of the ODN. Depending on different applications, a MIN may be located at the same place with the optical splitter. Each MIN is at least composed of an optical amplifier (OA) and an arrayed waveguide grating (AWG). The gain spectrum of the OA covers the wavelengths of the mobile signals. The AWG is used to route the signals at different wavelengths to different mobile sites. If a semiconductor optical amplifier (SOA) is used as the OA, the SOA and the AWG may be integrated into a single component [13]. An optical coupler may be further connected after the AWG to support more mobile sites providing the data rate per wavelength is sufficient. Here, a MIN can also act as a mobile site supporting different wireless modules (Mod). A wireless module may include a set of electrical processors, amplifiers, and antennas.

Due to the fiber chromatic dispersion, power fading occurs at different frequencies at different transmission distances. Fig. 2(a) and (b) show the power fading relationship between the transmission distances and chirp [16] induced from signal modulation. In our scheme, since external modulation is used and the bias current of laser source is fixed, negligible chirp is generated from the laser [17]–[19]. Hence, our chirp parameter is dominated by the MZM which in our analysis can be around 0.2. Since it is commercially available to have modulators with low chirps, chirp with  $\alpha$  up to 0.2 is considered. Even though the two arms of the MZM are respectively driven by complementary electrical signals, the power imbalance in the two arms (may be due to  $V_\pi$  drift [20]) can produce chirp. Since the  $V_\pi$  drift is typically in the range of 1–2 V, producing an overall power imbalance of about 70%, which can result in a chirp value of about 0.2. Hence, the scenarios of zero chirp and a chirp of 0.2 are considered here. The fiber dispersion parameters are calculated according to the Corning single mode fiber (Corning SMF-28 Optical Fiber). To obtain nearly equal signal performance for a system with differential distances up to 40 km (required for the NG-PON2), the 3-dB bandwidth after the fiber is regarded as the

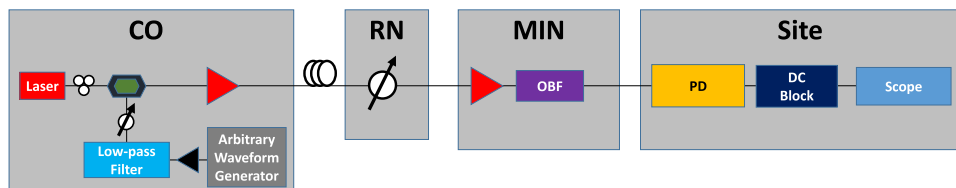


Fig. 3. Proof-of-concept experiment setup. CO: central office; RN: remote node; MIN: mobile intermediate node; OBF: optical band-pass filter; PD: photo-diode.

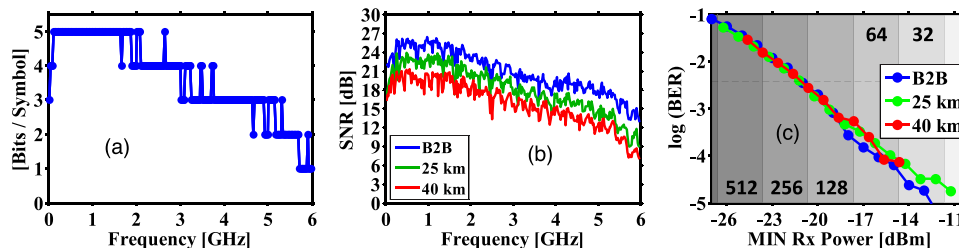


Fig. 4. Signal characteristics and performance. (a) Bit-loading scheme. (b) SNR response. (c) BER performance and split ratio.

available bandwidth for the transmission. Fig. 2(c) shows the relationship between the BER and the signal-to-noise ratio (SNR) under noise with Gaussian behavior, and Fig. 2(c) is independent of the chirp parameters. We can see for BER lower than the forward error correction (FEC) threshold ( $3.8 \times 10^{-3}$ ), the SNR penalty between the hierarchically neighboring formats is around 3–4 dB. Hence, by ensuring the power fluctuation among different subcarriers being less than 3 dB, similar performance will be obtained for signals with different transmission distances under a specific bit-loading scheme. Then, from Fig. 2(b), while the highest chirp is  $\alpha = 0.2$ , the available bandwidth for 40 km differential distances is about 6 GHz. This will be set as the system bandwidth for our mobile backhaul network.

### 3. Experimental Results and Discussion

Fig. 3 is the proof-of-concept experiment setup. A laser was launched into the Mach–Zehnder modulator (MZM) through a polarization controller (PC). The MZM was driven by OFDM signals generated by an arbitrary waveform generator. The sampling rate of the arbitrary waveform generator was 12 GS/s. The OFDM signals had their fast Fourier transform (FFT) size of 512, and 1/32 cyclic prefix (CP) was added in each OFDM symbol. The direct current (DC) component of the OFDM signal was not used, and the remaining 255 subcarriers were bit-loaded according to the system response. Fig. 4(a) shows the bit-loading scheme, which was unified for all different transmission distances. The net data rate of the signals was about 20.17 Gb/s. After the MZM, the optical signal was amplified by an erbium-doped fiber amplifier (EDFA). After 40 km transmission, the fiber output power was about  $\sim 3$  dBm. The termination node of the fibers was connected with the remote node (RN). An optical attenuator was used to emulate the power splitter. After the optical attenuator, the signals were amplified in the MIN and routed by an optical band-pass filter (OBF). In the mobile site, a PD was used to transform the optical signals into electrical signals. The DC component of the electrical signals was filtered by a DC block and input into a real-time sampling scope. The scope sampling rate was 40 GS/s. The received discrete signals were decoded offline.

Fig. 4(b) shows the SNR performance at different frequencies for different transmission distances while the optical attenuator was set 24 dB, which represents the split ratio requirement of NG-PON2 as 1:256. We can observe that the SNR curves shift nearly vertically for different transmission distances. This is a result of reduced power fading influence within our



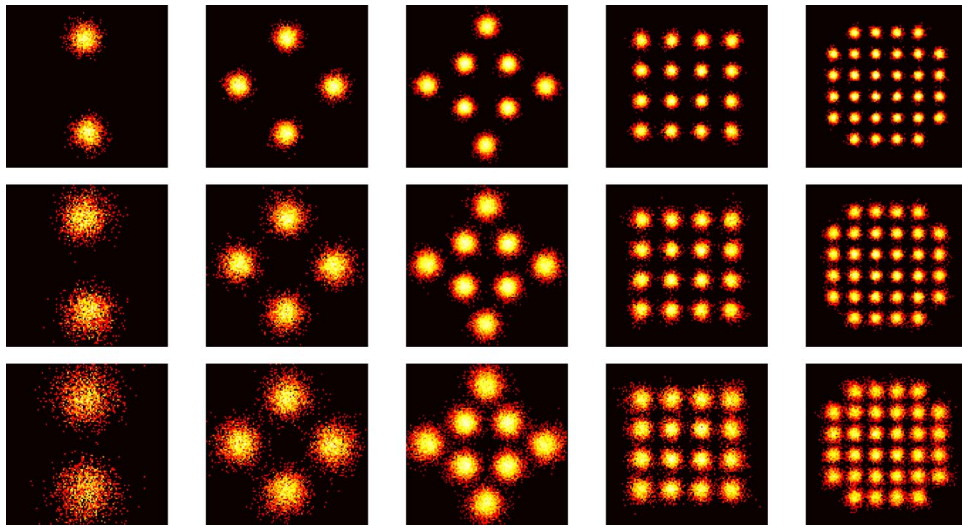


Fig. 5. Signal constellations. The first row: B2B; the second row: 25 km; the third row: 40 km.

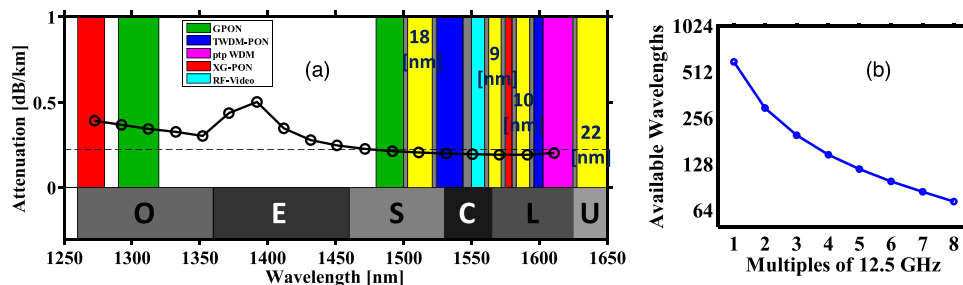


Fig. 6. Available wavelength analyses. (a) Wavelength plan. (b) Available wavelengths at different AWG channel grids.

transmission bandwidth. Fig. 4(c) shows the BER performance for different receiving power at the MIN. The corresponding split ratio at different Rx power was labeled with different bars with scaled gray colors. The dash line is the FEC threshold ( $BER = 3.8 \times 10^{-3}$ ). The split ratio of 256 with BER less than the FEC threshold can be achieved. Fig. 5 shows the corresponding constellation of different transmission distances with 256 split ratio. From top to the bottom, different rows are, respectively, the constellations of B2B, 25 km, and 40 km.

In our proof-of-concept demonstration, we show that each wavelength can support about 20 Gb/s (net data rate is 20.17 Gb/s), which corresponds to spectral efficiency of 3.36 b/s/Hz. Considering the capacity requirement of IMT-A (1 Gb/s) [14], LTE-A (currently 3 Gb/s) [15], and 5G (expectedly  $> 10$  Gb/s) [1], [2], we can see that the estimated supported nodes of the mobile systems are respectively 20, 6, and 2 for each wavelength. In the migration stage from the 4G systems into the 5G systems, it may be also inevitable to have the new 4G nodes and 5G nodes deployed at the same time. Then the LTE-A nodes and the 5G nodes can also be developed in the ratio of 3:1 for each wavelength. This hybrid system can be used for developing the 5G systems in the preliminary stage.

Fig. 6(a) shows the attenuation response of ITU-T G.652 fiber [6], with the wavelength allocation for the existing services is shown in the figure legends of [21, Fig. 6(a)]. According to Fig. 4(c), after 40 km transmission, there remains less than 1 dB power budget for 256 split-ratios satisfying the FEC threshold; hence, the allowable fiber attenuation should be less than 0.225 dB/km to support 40 km transmission. The attenuation of 0.225 dB/km is marked by the dash line of Fig. 6(a). Besides, guard bands of 3 nm are reserved for each application; hence, only the wavelength band with yellow color shown in Fig. 6(a) are available, and the total

available bandwidth is about 59 nm ( $18 + 9 + 10 + 22$  nm). For different grids of the AWG used, the estimated available mobile nodes will be 20, six, and two nodes respectively for the IMT-advanced, current LTE-A systems, and the expected 5G systems. The scaling factor is shown in Fig. 6(b) according to the AWG grid unit of 12.5 GHz. Even with 100 GHz ITU grid, 73 DWDM channels are available for our proposed integrated systems.

#### 4. Summary

An integration scheme of running the OFDM based mobile backhaul networks over the existing PON systems is proposed and demonstrated. In our proposed scheme, the expense for deploying new fibers for the mobile backhaul networks can be reduced. Hence, it meets the cost reduction requirement for developing emerging 5G systems. Moreover, in our proposed scheme, we do not need to adaptively adjust the transmitted OFDM signal according to different distances between the end nodes and the CO; hence, the signal process time can be further reduced. From our experiment results, we successfully demonstrated the integration systems with 256 split ratio and, at most, 40 km transmission distance, which meets the requirement of NG-PON2. 20.17 Gb/s net data rate was also demonstrated to support 20, six, and two nodes/wavelength, respectively, for the requirement of the IMT-advanced, current LTE-A systems, and the expected 5G systems.

---

#### References

- [1] J. G. Andrews *et al.*, "What will 5G be?" *IEEE J. Sel. Areas Commun.*, vol. 32, no. 6, pp. 1065–1082, Jun. 2014.
- [2] "5G white paper- 5G radio access: Requirements, concepts and technologies," NTT Docomo, Tokyo, Japan, White Papers, Jul. 2014.
- [3] K. Casier *et al.*, "A clear and balanced view on FTTH deployment costs," in *Proc. FITCE Congr.*, London, U.K., 2008, pp. 109–112, Paper 02.
- [4] C. H. Chang *et al.*, "An integrated long-reach PON and GI-POF in-house network architecture for hybrid CATV/OFDM signals transmission," *J. Lightw. Technol.*, vol. 30, no. 20, pp. 3247–3251, Oct. 2012.
- [5] C. Li, W. Guo, W. Hu, and M. Xia, "Energy-efficient dynamic bandwidth allocation for EPON networks with sleep mode ONUs," *Opt. Switch. Netw.*, vol. 15, pp. 121–133, Jan. 2015.
- [6] *40-Gigabit-Capable Passive Optical Networks (NG-PON2): General Requirements*, ITU-T Recommendation G.989.1, Mar. 2013.
- [7] N. Cvijetic, "OFDM for next-generation optical access networks," *J. Lightw. Technol.*, vol. 30, no. 4, pp. 384–398, Feb. 2012.
- [8] I. C. Lu *et al.*, "20-Gbps WDM-PON transmissions employing weak-resonant-cavity FPLD with OFDM and SC-FDE modulation formats," *Opt. Exp.*, vol. 21, no. 7, pp. 8622–8629, 2013.
- [9] Y. C. Chi *et al.*, "Optical 16-QAM-52-OFDM transmission at 4 Gbit/s by directly modulating a coherently injection-locked colorless laser diode," *Opt. Exp.*, vol. 20, no. 18, pp. 20071–20077, 2012.
- [10] W. R. Peng, I. Morita, H. Takahashi, and T. Tsuritani, "Transmission of high-speed (> 100 Gb/s) direct-detection optical OFDM superchannel," *J. Lightw. Technol.*, vol. 30, no. 12, pp. 2025–2034, Jun. 2012.
- [11] C. W. Chow, C. H. Yeh, and J. Y. Sung, "OFDM RF power-fading circumvention for long-reach WDM-PON," *Opt. Express*, vol. 22, no. 20, pp. 24392–24397, Sep. 2014.
- [12] C. H. Yeh, C. W. Chow, H. Y. Chen, and B. W. Chen, "Using adaptive four-band OFDM modulation with 40 Gb/s downstream and 10 Gb/s upstream signals for next generation long-reach PON," *Opt. Exp.*, vol. 19, no. 27, pp. 26150–26160, Dec. 2011.
- [13] H. Ishii and Y. Yoshikuni, "InP-based photonic integrated devices consisting of arrayed waveguide grating and semiconductor optical amplifiers," presented at the Opt. Amplifiers Their Applicat. Conf., Jul. 1, 2001, Paper OTuC4-1.
- [14] *Detailed specifications of the terrestrial radio interfaces of International Mobile Telecommunications-Advanced (IMT-Advanced)*, ITU-R Recommendation M.2012-1, Feb. 2014.
- [15] [Online]. Available: <http://www.3gpp.org/technologies/keywords-acronyms/97-lte-advanced>
- [16] F. Devaux, Y. Sorel, and J. F. Kerdiles, "Simple measurement of fiber dispersion and of chirp parameter of intensity modulated light emitter," *J. Lightw. Technol.*, vol. 11, no. 12, pp. 1937–1940, Dec. 1993.
- [17] C. H. Henry, "Theory of the linewidth of semiconductor lasers," *IEEE J. Quantum Electron.*, vol. QE-18, no. 2, pp. 259–264, Feb. 1982.
- [18] A. Villafranca, J. A. Lázaro, I. Salinas, and I. Garcés, "Measurement of the linewidth enhancement factor in DFB lasers using a high-resolution optical spectrum analyzer," *IEEE Photon. Technol. Lett.*, vol. 17, no. 11, pp. 2268–2270, Nov. 2005.
- [19] C. J. Lin and G. R. Lin, "Frequency chirp and mode partition induced mutual constraint on the side-band phase noise of a mode-locking WRC-FPLD fiber ring self-started with a lengthened feedback loop," *Laser Phys.*, vol. 23, no. 4, 2013, Art. ID 045103.
- [20] J. Švarný, "Analysis of quadrature bias-point drift of Mach–Zehnder electro-optic modulator," in *Proc. Biennial BEC*, 2010, pp. 231–234.
- [21] *40-Gigabit-Capable Passive Optical Networks 2 (NG-PON2): Physical Media Dependent (PMD) Layer Specification*, ITU-T Recommendation G.989.2, Dec. 2014.